Chaotic Mixing of Two Similar Fluids in the Presence of a Third Dissimilar Fluid

D. F. Zhang and D. A. Zumbrunnen
Laboratory for Materials Processing and Industrial Mixing and Materials Science and Engineering Program, Dept. of Mechanical Engineering, Clemson University, Clemson, SC 29634

Two-dimensional chaotic mixing of similar Newtonian fluids in the presence of an advected dissimilar minor phase fluid body with specified size, interfacial tension, and viscosity ratio was numerically investigated. Interfacial tension was sufficiently high to allow only small deformations in the dissimilar minor phase body. Mixing was confined to a rectangular cavity with periodically driven upper and lower surfaces. Regions of regular motion (i.e., islands) of comparable size to the minor phase body were eventually destroyed or replaced by the minor phase body. Islands persisted for longer times when the initial separation distance between the minor phase body and island was large or when the viscosity ratio was small. When interfacial tension was small enough to deform the minor phase body more readily, islands showed little indication of instability. Results suggest opportunities for improving mixing uniformity in practical processes and disclose how interactions between dissimilar fluids affect mixing.

Introduction

Studies have been performed in recent years of the chaotic motion of fluid particles within periodically driven cavity flows. All of these motions yield recursive stretching and folding in minor phase bodies and thereby serve as useful models of mixing. Investigations of chaotic mixing have largely involved similar fluids where interfacial forces can be neglected and where immiscibility can be assumed. In contrast, interfacial tension and shear forces may be present at interfaces between dissimilar fluids. Investigations with similar fluids have elucidated the kinematics of mixing and established research methodologies that can be applied to more general mixing conditions where interfacial forces are important. Much of the initial work has been summarized by Ottino (1989). Experiments and numerical simulations (Chien et al., 1986; Leong and Ottino, 1989) have revealed the existence of poorly mixed regions, where fluid particle motion was regular, surrounded by well-mixed regions in which chaotic advection occurred. The poorly mixed regions have been appropriately designated as "islands," and were found to coexist with the well-mixed regions for large times for some protocols of wall motion. Surfaces of such islands in two-dimensional cavity flows are physical representations of KAM curves, which are predicted by the Kolmogorov–Arnold–Moser theorem (Lichtenberg and Liebermann, 1992). According to this theorem, regions of regular behavior can coexist with chaotic regions in Hamiltonian (i.e., conservative) systems of two degrees of freedom.

As a means to counter island formation in a driven cavity, Leong (1990) proposed placing fixed internal obstructions within the cavity to obtain a more complex flow field. Jana et al. (1994) extended this concept and designed a rectangular cavity into which baffles were periodically inserted and withdrawn. The actions of such movable baffles were effective in promoting uniform mixing conditions. The obstructions or movable baffles have some relation to the advected minor phase bodies of this study. In all of these cases, the flow field in the major phase fluid is altered. Based on the results of Jana et al. (1994), it is reasonable to anticipate that the presence of minor phase bodies may destabilize islands and thereby lead to improved mixing conditions in regions of the cavity occupied by similar fluids.

Liu et al. (1994b) examined in detail the stretching fields in a rectangular cavity filled with a single fluid to assess mixing efficiencies. Stretching was measured as the deformation in a population of advected material elements scattered throughout the cavity referenced to a very small initial length. The locations of islands were apparent in maps of the stretching fields and corresponded closely with those in numerically

Correspondence concerning this article should be addressed to D. A. Zumbrunnen.

generated patterns of advected particles. Interestingly, effective stretching was disclosed near some islands due to the actions of nearby unstable manifolds of periodic hyperbolic points.

Parameters of most earlier chaotic mixing studies have been chiefly associated with cavity geometry or prescribed motions at the cavity walls, since mixing has been performed with similar fluids. Some initial studies of chaotic mixing of dissimilar fluids or fluids and added particles have been reported recently. Tjahjadi and Ottino (1991) documented deformations in droplets under chaotic mixing conditions in a fluid contained between two eccentric rotating cylinders. Droplets of high viscosity experienced more stretching since interfacial instabilities instilled by internal fluid motion arose less rapidly than in droplets of low viscosity. Breakup of filaments occurred preferentially near folds where stretching was abated and ultimately led to the formation of small droplets that were dispersed by chaotic advection throughout the flow domain. Conditions for breakup of similar filaments within quiescent fluids was disclosed in a numerical and experimental study by Tjahjadi et al. (1992), and have been discussed in a review by Stone (1994). Chaotic mixing of a single-phase fluid with added solid particles was considered by Liu et al. (1994a) within a rectangular cavity. The influence of the particles on the flow field and particle interactions were not considered. The motion of the solid particles was shown to be governed by a nonconservative (i.e., dissipative) system of equations in contrast to the fluid motion that was governed by a conservative system. Consequently, the motions of solid particles can trace out strange attractors within Poincaré sections and can cross KAM curves in fluid advection patterns. Recently, a numerical model of two-phase cavity flows was developed by Zhang and Zumbrunnen (1996). Difficulties associated with determining the locations of moving interfaces between phases of complex shapes were overcome by implementing the volume of fluid (VOF) method (Hirt and Nichols, 1981) developed for free surface flows in combination with a recently developed continuum surface force (CSF) method (Brackbill et al., 1992) for interfacial force representation. A numerically efficient algorithm was obtained, since interface reconstruction was not required to prescribe interfacial forces during computations. Interactions between multiple minor phase bodies and the effects of viscosity ratio and interfacial tension on interfacial morphology were investigated under chaotic mixing conditions for short mixing intervals. Chakravarthy and Ottino (1996) employed a modified marker-and-cell method to study the stretching of initially round or layered minor phase bodies of specified viscosity in a lid-driven rectangular cavity. Interfacial-tension forces were neglected, since results pertaining to high capillary numbers were of interest. Results illustrated the importance of properly locating feed locations in mixing devices and the relation of stretching to the velocity field.

The chaotic mixing studies by Tjahjadi and Ottino (1991) and Zhang and Zumbrunnen (1996) investigated stretching and breakup of droplets, but the influence of the droplets themselves on the chaotic mixing environment was presumed to be negligible. Since two or more phases are combined in actual mixing processes, interfacial forces are commonly present. The influences of interfacial forces must therefore also be investigated as part of an overall effort to obtain an improved understanding of mixing. Mixing with active interfaces is a complex process in which interfacial-tension and interfacial-flow stresses modify the flows within all phases as well as the interfaces themselves. Minor phase bodies with capillary numbers above a critical value can experience progressively decreasing dimensions as mixing proceeds (Muzzio et al., 1991), so that numerical simulations eventually become untenable. However, numerical modeling of multiphase chaotic mixing has become possible in recent years as a result of new methodologies and faster digital computers for situations where reductions in length scales of minor phase bodies are not large or where short mixing intervals are of interest. A primary motivation for the prior work by Zhang and Zumbrunnen (1996) was to provide insights in support of ongoing research to produce directly fine-scale composite materials and advanced polymer blends by chaotic mixing of melts (Zumbrunnen et al., 1996; Liu and Zumbrunnen, 1996). Uniformity in microstructures that are derived from interfacial morphologies upon solidification is an important objective of this novel melt-processing technique, so islands in melts are undesirable. In this article, the influence of an advected dissimilar minor phase fluid body of specified interfacial tension and viscosity ratio on chaotic mixing between two similar fluids is investigated numerically. In addition to systematic evaluations of grid size and time step sensitivities, the numerical procedures were validated by comparison of predictions to experimental results and by comparison to prior experimental and theoretical results for mixing studies of similar fluids. Numerical consideration of large mixing times was possible in this study since computations were performed for interfacial tensions that oppose significant stretching of the dissimilar minor phase fluid body. Although the present study has broad application to mixing in general, an understanding is gained of island stability in the presence of minor phase bodies that may be useful in producing multiphase materials by melt processing with more uniform microstructures.

Numerical Modeling

Numerical modeling was performed under conditions pertaining to the following assumptions: (1) unsteady, laminar flow; (2) constant properties; (3) similar fluids A and C and dissimilar fluid, B; (4) immiscible and incompressible, Newtonian fluids A, B, and C; (5) no-slip conditions at both cavity walls and fluidic interfaces; (6) absence of gravitational or other external body forces. The computational domain and applicable velocity boundary conditions are shown in Figure 1. The computational domain was of a two-dimensional rectangular cavity resembling the one in chaotic mixing studies performed by other researchers (Leong and Ottino, 1989; Liu et al., 1994a). The upper and lower walls moved according to assigned velocity functions $u_T(t)$ and $u_B(t)$. The lateral walls were fixed. A discontinuous velocity protocol, in which the upper wall moved for one-half time period while the lower wall was stationary followed by an identical motion in the opposite direction by the lower wall, was selected since chaotic particle motion can be achieved under this period flow condition (Leong and Ottino, 1989). A fluid B minor phase body, with mass density ρ_B and viscosity μ_B, was initially suspended in the major phase fluid A of mass density ρ_A and viscosity μ_A. The initial sizes and initial locations of the fluid

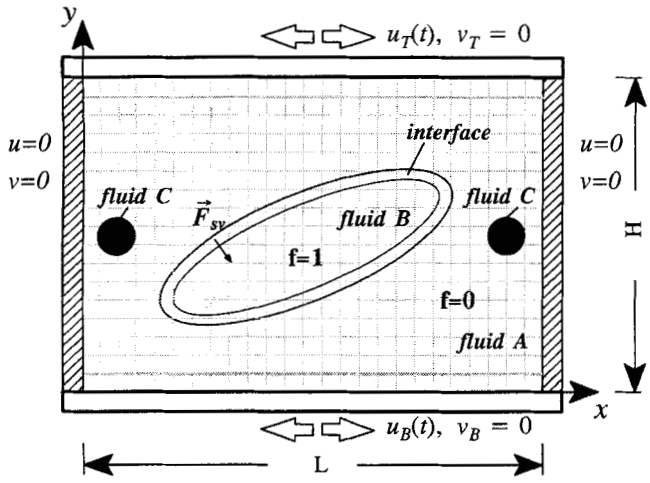

Figure 1. Computational domain and boundary conditions employed in the numerical model.

B minor phase bodies were specified. In Figure 1, the two black minor phase bodies (fluid C) had passive interfaces with respect to the surrounding major phase fluid A and therefore served as tracers. Thus, fluid B was dissimilar to similar fluids A and C. Circular shapes were specified as the initial shapes of all minor phase bodies. Fluid C bodies had initial diameters of $0.05L$ and comprised 20,000 uniformly distributed particles. The positions of these particles were calculated from the velocity field to discern the extent of mixing external to fluid B. A description of the tracking algorithm will be described later. Ranges of initial diameters and initial locations as well as interfacial properties for fluid B were considered.

Numerical simulations of chaotic mixing of fluids with active interfaces involve the solution of the Navier–Stokes equations for two or more fluid phases with specified boundary and interfacial conditions. The major difficulties lie in the unknown locations of the deforming, moving fluidic interfaces, which must be found together with the pressure and velocity fields within the different fluid phases. A comprehensive review was conducted of both established and recently developed approaches (Zhang and Zumbrunnen, 1996; Zhang, 1996). A primary goal has been to construct a numerical model capable of simulating the evolution during mixing of minor phase bodies of simple initial shapes into minor phase bodies with interfaces of complex shapes. With regard to locating the interface, the VOF method (Hirt and Nichols, 1981) was selected since it overcomes ambiguities in interface location and computational inefficiencies inherent in other methods by associating with the interface one scalar function $f(X, Y, t)$. The function f was defined as the fractional volume of a computational cell occupied by the minor phase fluid B. Cells with f values between zero and one then identified interface locations. Thus, the VOF method provided the same interface information available from other methods, which commonly track the position of massless marker particles within each phase or the interface itself, but computational storage requirements were consistent with requirements for all other dependent variables. The two-dimensional evolution equation of f was obtained by noting that f is in essence an advected quantity and is thereby governed by the equation $Df/Dt = 0$. A discretization equation was obtained from this equation with the finite-volume approach, which included the change of f over a computational cell and the volumetric flow of fluid B across the finite volume. Since f changes abruptly over the interface from zero to unity, changes were calculated according to the donor–acceptor algorithm described by Hirt and Nichols (1981).

Reconstruction of interfaces is often performed at each time step in order to determine and assign interfacial forces. Such reconstructions are computationally expensive. Recently, a two-dimensional CSF technique for modeling interfacial tension was introduced by Brackbill et al. (1992). In this method, interfacial tension is interpreted as a continuous, three-dimensional effect across an interface, rather than a boundary condition on the interface. Interfacial forces can thereby be replaced by an equivalent volumetric force. As a consequence, the CSF technique is ideally suited for Eulerian interfaces that are not in general aligned with the computational grid. Moreover, volumetric forces from the CSF technique can be expressed in terms of the function f of the VOF method, so interface reconstruction is unnecessary. Details of CSF technique are available in recent papers (Kothe et al., 1991; Richards et al., 1992; Zhang and Zumbrunnen, 1996; Zhang, 1996).

With interfacial forces obtained with the VOF method and the CSF technique, the continuity equation and the momentum equations in Cartesian coordinates were nondimensionalized in terms of suitable dimensionless parameters and variables (see Notation). Since modeling was performed under creeping flow conditions, the scale factor P_0 for pressure relates to viscous forces instead of inertial forces, for example. Additionally, the steady speeds of the upper and lower walls were used to scale velocities, and the mixing period T and cavity length L defined a dimensionless frequency in terms of a Strouhal number St. A parameter σ_B^* denoted a dimensionless interfacial tension and differs from an inverse capillary number, since a local viscous shear stress and a drop size were not used in its derivation. The resulting dimensionless equations are given below:

$$\frac{\partial U}{\partial X} + \frac{1}{A}\frac{\partial V}{\partial Y} = 0 \tag{1}$$

$$StRe\left(\frac{\partial (MU)}{\partial \tau} + U\frac{\partial (MU)}{\partial X} + \frac{1}{A}V\frac{\partial (MU)}{\partial Y}\right) = -\frac{\partial P}{\partial X} + \frac{\partial}{\partial X}\left(\Gamma\frac{\partial U}{\partial X}\right) + \frac{1}{A^2}\frac{\partial}{\partial Y}\left(\Gamma\frac{\partial U}{\partial Y}\right) + \sigma_B^* K\frac{\partial f}{\partial X} \tag{2}$$

$$StRe\left(\frac{\partial (MV)}{\partial \tau} + U\frac{\partial (MV)}{\partial X} + \frac{1}{A}V\frac{\partial (MV)}{\partial Y}\right) = -\frac{1}{A}\frac{\partial P}{\partial Y} + \frac{\partial}{\partial X}\left(\Gamma\frac{\partial V}{\partial X}\right) + \frac{1}{A^2}\frac{\partial}{\partial Y}\left(\Gamma\frac{\partial V}{\partial Y}\right) + \frac{1}{A}\sigma_B^* K\frac{\partial f}{\partial Y}. \tag{3}$$

The dimensionless mass density M and viscosity Γ in Eq. 2 and Eq. 3 are properties of computational cells in which both fluid A and fluid B may be contained. Given the fact that the sharp A/B interface is replaced with the CSF technique by a transition region, these two properties were obtained by

linearly combining the properties of two different fluids according to the volume fraction f:

$$M = 1 + f(C_\rho - 1) \tag{4}$$

$$\Gamma = 1 + f(C_\mu - 1). \tag{5}$$

Physically appropriate boundary conditions were specified at the cavity walls as shown in Figure 1. Protocols for the wall velocities u_T and u_B to give chaotic mixing conditions were discussed earlier. Equations 2 and 3 were discretized using the finite volume approach and were solved according to the SIMPLE method (Patankar, 1980). A uniform mesh was used in both the X and Y directions. A fully implicit formulation, using first-order backward differencing for temporal terms, was used to avoid instability problems. The hybrid scheme (Spalding, 1972) was used to discretize advective and diffusive terms. Pressures and velocities in each mesh cell were adjusted iteratively by the successive overrelaxation method to satisfy continuity (Eq. 1). This iteration process continued until convergence criteria (see below) were satisified in the entire computational domain. Based on the convergent velocity field, the donor–acceptor algorithm (Hirt and Nichols, 1981) was used to update the fractional f values in the VOF method.

Since the interface between similar fluids A and C was passive, positions of fluid C particles were calculated directly by integration of Eq. 6 from the resolved velocity field V within fluid A:

$$\frac{dX}{d\tau} = V, X(\tau = 0) = X_0. \tag{6}$$

In Eq. 6, V was interpolated between grid points using a biquadratic scheme from the converged velocity field. Integration was conducted by the second-order Runge–Kutta algorithm.

The local extent of mixing can be expressed in terms of the deformation of small bodies. Such deformations are related to Lyapunov exponents for the mixing process and can be expressed in terms of stretching rates as described by Ottino (1989) and implemented recently by Liu et al. (1994b). Stretching rate was calculated by determining the distance of four neighboring particles from a fiduciary particle after the completion of successive mixing periods. With the four particles initially placed symmetrically a small distance $l_0 = 10^{-6}L$ from the fiduciary, the subsequent positions of all particles, including the fiduciary, were determined. The stretching rate λ was defined by

$$\lambda = |l|/|l_0|, \tag{7}$$

where l was the distance between the fiduciary and a neighboring particle after a specified number of mixing periods. In order to obtain detailed plots of the stretching field within the entire mixing cavity, 200×120 fiduciary particles were uniformly distributed in the mixing cavity, which provided 96,000 values of λ. This number of values provided clear plots of the stretching field, but was less than the number employed by Liu et al. (1994b) in their mixing study of fluids with passive interfaces in an identical cavity. A somewhat coarser stretching field was constructed here to keep particle tracking computations tenable since it was necessary to evaluate the instantaneous velocity fields owing to interfacial motions.

The grid was successively refined to ensure grid independence in the calculated instantaneous velocity fields, an acceptably small numerical uncertainty in the calculated positions of interfaces after the maximum number of mixing periods ($N = 20$), and correctly disclose features of the mixing process. Detailed information has been presented by Zhang (1996). Calculated steady velocity components at nine unique reference points were compared. For grids of 50×30, 80×48, and 100×60 in the X and Y directions, relative differences in velocity components decreased from 0.85 to 0.10%. Interface locations were more sensitive to grid size than was the velocity field, since errors can accumulate over many time steps, as pointed out by Souvaliotis et al. (1995). To assess the effect of grid size on interface location, a fluid B body ($d_0 = 0.16L$) was placed initially at the center of the cavity and mixing was simulated in the cavity with $St = 0.16$. For the preceding meshes, relative differences decreased upon grid refinement from $0.06d_0$ to $0.03d_0$. The 100×60 mesh was selected to obtain reasonable run times and permit a comprehensive study since typical run times increased from about 16 hours to about 60 hours with the 150×90 mesh on a Silicon Graphics, Inc. (Mountain View, CA) Onyx supercomputer (75 MFLOP). Time-step independence for both velocity and particle locations was assessed by successively refining the time step $\Delta\tau$ until calculated values at each time step for the selected grid size had relative differences of less than 10^{-5}. For most cases, $\Delta\tau = 10^{-3}$ was selected. With this time step, numerically generated particle trajectories over times comparable to those in the mixing results formed closed loops as required when a steady flow field was generated with only one wall of the mixing cavity in motion.

Several available solutions were used to assess accuracy and further validate the numerical model with the selected 100×60 mesh and time step $\Delta\tau = 10^{-3}$. Steady flow fields in the cavity of Figure 1 with one wall moving and the other wall stationary or with two walls simultaneously moving were solved. Striation patterns under chaotic mixing conditions for $N = 6$ were also generated by tracking 20,000 fluid particles composing a small passive fluid body. Predicted streamlines and striation patterns appeared identical upon visual comparison to photographs of the corresponding experimental results reported by Leong and Ottino (1989). The VOF algorithm was assessed by comparing the calculated interface locations to that given by particle tracking with passive interfaces, and excellent agreement was found. As stated earlier, for the maximum number of mixing periods considered ($N = 20$), both particle and interface locations were determined within $0.06d_0$ based on successive grid refinement. Moreover, the general features of the mixing environments for the finest grids were similar. Such similarities in numerical mixing simulations for various grid sizes have been demonstrated recently by Souvaliotis et al. (1995). The VOF results were also compared and found to be in excellent agreement with the experimental results of deformed passive tracers in steady cavity flows obtained by Chien et al. (1986). An example given by Brackbill et al. (1992) was used to test the CSF algorithm.

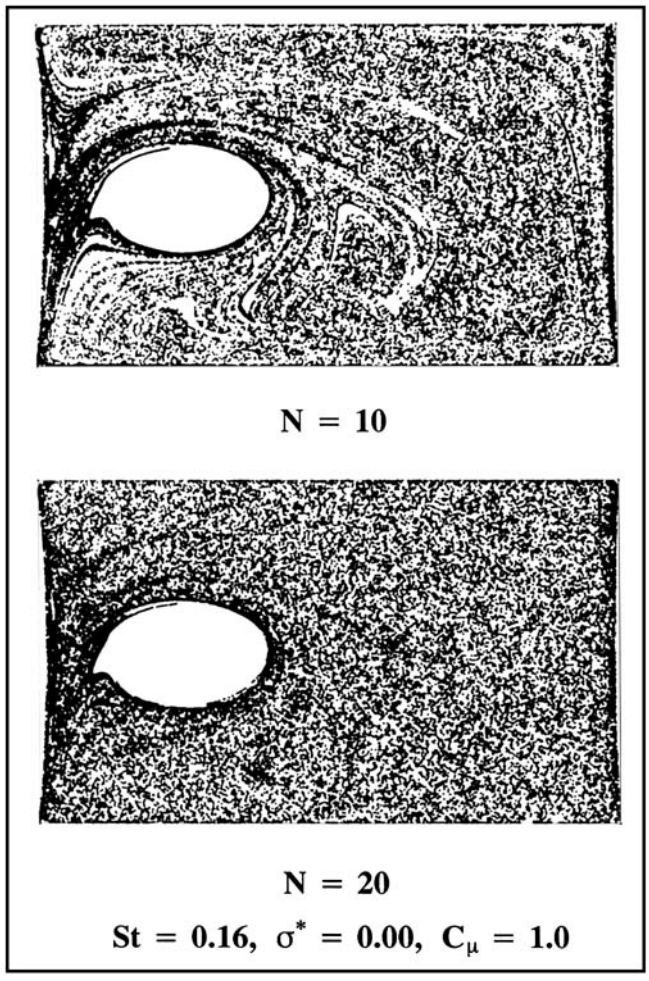

Figure 2. Positions of similar fluid *C* particles within fluid *A* without the dissimilar fluid *B* minor phase body for $A = 0.6$, $StRe = 1$, and (a) $N = 10$, (b) $N = 20$.

The surface-tension-driven flow for an initially square blob within a quiescent fluid was used and the equilibrium circular form was correctly predicted. Further validation of the CSF algorithm was conducted by direct comparisons to the experimental measurements of drop deformations by Bentley and Leal (1986). Numerical predictions of interfacial locations and pressure distributions in extended drops at different times were also compared to the numerical results of Stone and Leal (1989). In all cases, good agreement was obtained (Zhang, 1996). It should be noted that the two finest grids yielded similar results regarding island formation and stability. Since the general features of the mixing environments for the finest grids were also similar as stated before, improved understanding of mixing processes with active interfaces can be obtained numerically even when interface locations are subjected to accumulated computational error.

Results and Discussion

In order to establish baseline results and facilitate subsequent examinations of the influences of the deforming fluid B minor phase body (Figure 1), the mixing conditions in the cavity with only two, similar ($\sigma_C^* = 0$, $C\mu_C = 1$) fluid C minor phase bodies were investigated. These bodies were placed initially at $(x_1, y_1) = (0.08L, 0.5H)$ and $(x_2, y_2) = (0.85L, 0.5H)$ and had a $0.05L$ diameter. As has been described, mixing conditions throughout this investigation pertained to oppositely directed and alternately moving upper and lower cavity walls over a time period T. A dimensionless frequency of this driven flow can be expressed in terms of the Strouhal number St ($= L/Tu_0$). With $St = 0.16$, Leong and Ottino (1989) demonstrated experimentally that a large island is formed surrounded by a continuous region of chaotic mixing. The numerically determined locations of the passive particles that make up the similar fluid C minor phase bodies are given in Figure 2 at the completion of 10 and 20 periods, and are in excellent agreement with their results. It is apparent that the large island was well defined after 10 periods and persisted in the cavity at the conclusion of 20 periods. Since the mixing process is Hamiltonian (Aref, 1984), the island boundary is a physical representation of a KAM curve (Lichtenberg and Liebermann, 1992). Fluid C particles therefore cannot cross the island boundary, and the volume of fluid A within the island thus remains unmixed with fluid C. Simulations with $St = 0.16$ were ideal for detecting the influence of dissimilar fluid B on island stability and was therefore specified for all subsequent figures. With fluid B present in the cavity, the mixing process may be regarded as one involving three immiscible fluids, where fluid A and fluid C are similar and fluid B is dissimilar. Comparisons of subsequent figures with Figure 2 thereby demonstrate the effect of fluid B on mixing of similar fluids A and C. Careful selection of parametric conditions was necessary in order to perform a systematic study efficiently with fluid B. Values of σ_B^* and $C_{\mu B}$ were thereby varied only over ranges where island stability differed. Computations were performed for $0.25 < \sigma_B^* < 1.0$ and $0.5 < C_{\mu B} < 10.0$. It should be noted that the applicability of σ_B^* to a particular fluid depends on the mixing rate, since σ_B^* was referenced to the speed of the moving walls of the cavity. Since the effects above and below the maximum and minimum specified values of σ_B^* and $C_{\mu B}$ were qualitatively similar, it is possible to discern from the subsequent figures the results for values outside of the selected ranges.

The influence of an advected deformable minor phase body of fluid B (Figure 1) on chaotic mixing is considered in Figure 3. This minor phase body was initially circular with diameter $0.16L$, and was initially placed at the location of the island shown in Figure 2 [i.e., $(x_0, y_0) = (0.25L, 0.5H)$]. Interfacial tension and viscosity ratio were specified that yield only small deviations from the initial circular shape. Two passive minor phase bodies of fluid C were also present in the cavity at the same locations and of the same diameters specified for Figure 2. Locations of passive fluid C particles are shown in Figure 3 at the completion of the indicated number of mixing periods. Results without fluid B are shown in the left column, while results with fluid B for otherwise identical conditions are shown in the right column. It was clearly observed that the minor phase body (fluid B) moved within the cavity as an autonomous body due to the high values specified for interfacial tension and viscosity ratio. As demonstrated by Zhang and Zumbrunnen (1996), velocity fields in the vicinity of strong interfaces can significantly modify the local velocity field. The consequence of these modifications is

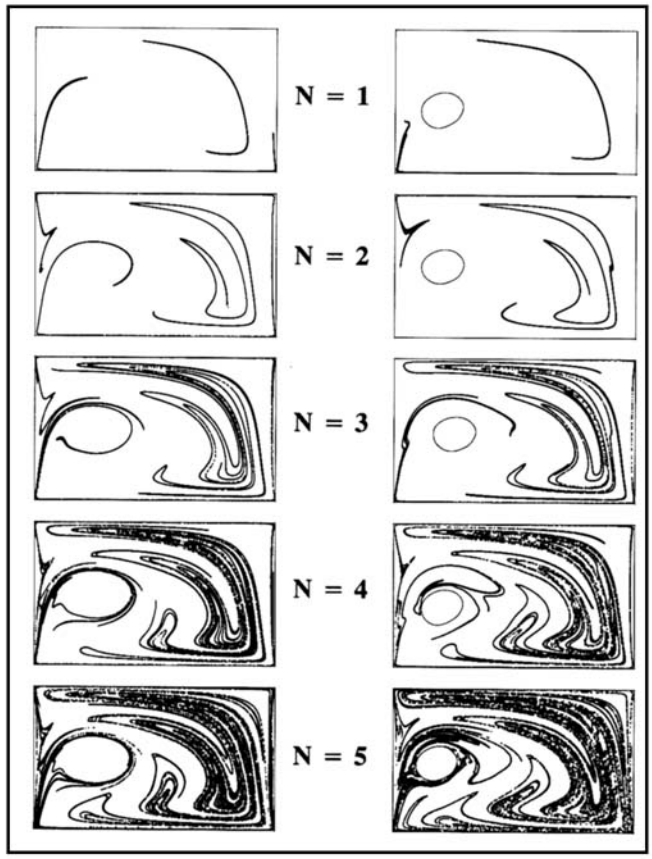

Figure 3. Island formation in similar fluids *A* and *C* (left) and replacement of island by dissimilar fluid *B* (right) with the fluid *B* minor phase body initially located at $(x_0, y_0) = (0.25L, 0.5H)$ and for $A = 0.6$, $\sigma_B^* = 1.0$, $C_{\mu B} = 10.0$, $d_0 = 0.16L$, $St = 0.16$.

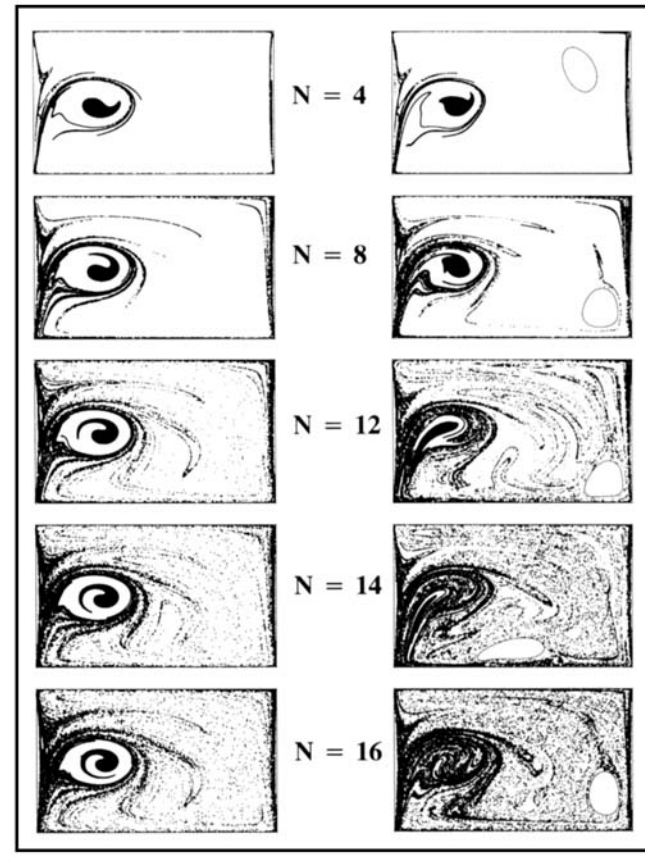

Figure 4. Island collapse due to advecting fluid *B* minor phase body initially located away from island with $A = 0.6$, $\sigma_B^* = 1.0$, $C_{\mu B} = 10.00$, $d_0 = 0.16L$, $St = 0.16$.

evident by comparing the dark advection patterns in the passive fluid C for $N = 2$ shown in both columns. The advection pattern beneath the fluid B minor phase body has been significantly altered. However, further from the fluid B minor phase body, little change is evident. The formation of the island of Figure 2 can be discerned in the left column for successive mixing periods. A striation in the advection pattern encircled a region of fluid A until a KAM curve was formed. However, in the right column, regions for chaotic mixing that existed in the upper, lower, and right regions of the cavity extended to the fluid B interface. In addition, the island was effectively replaced by the smaller fluid B minor phase body and the region for chaotic mixing was enlarged.

Figure 4 demonstrates a more general case in which the minor phase body of fluid B was initially placed at a location far from the eventual location of the island in Figure 2. In order to follow events most clearly, one similar fluid C tracer was located inside the island $[(x_0, y_0) = (0.25L, 0.5H)]$, while the other was located within the nearby chaotic region $[(x_0, y_0) = (0.08L, 0.5H)]$. As with Figure 3, the left column in Figure 4 shows results without fluid B present for comparison purposes. In the left column, the two similar fluid C tracers remained separated as expected. With the addition of fluid B, distortions in the island boundary occurred and are easily seen for $N = 4$. This disturbance was due to the alteration of the flow field by the motion of fluid B beyond the island. Disturbances in the island boundary were accompanied by disturbances in the flow field within the island, as evidenced by convolutions in the boundary between fluid B and fluid C. The continuing deformations in the advected fluid B body continued to disturb the island boundary and eventually led to the collapse of the island. Such *island collapse* due to the motion of suspended bodies is potentially useful in mixing processes. The minor phase body in this case may be regarded as a rigid, neutrally buoyant stirrer added to the cavity.

The island collapse of Figure 4 is clearly shown in Figure 5 as stretching fields at the completion of 20 mixing periods, where the upper panel corresponds to the case without the fluid B minor phase body. The stretching fields are color-coded and stretching, as defined earlier, increases in sequence from black, green, yellow and red. Corresponding ranges for λ are indicated in the caption. In the upper panel without the minor phase fluid body B, stretching rates were high throughout the mixing cavity due to chaotic mixing conditions except within the island where advection was regular. Similar numerical results were obtained previously by Liu et al. (1994b) in an identical cavity. In the lower panel, the advecting fluid B minor phase body is evident in the upper-right corner of the cavity. The high interfacial tension and high

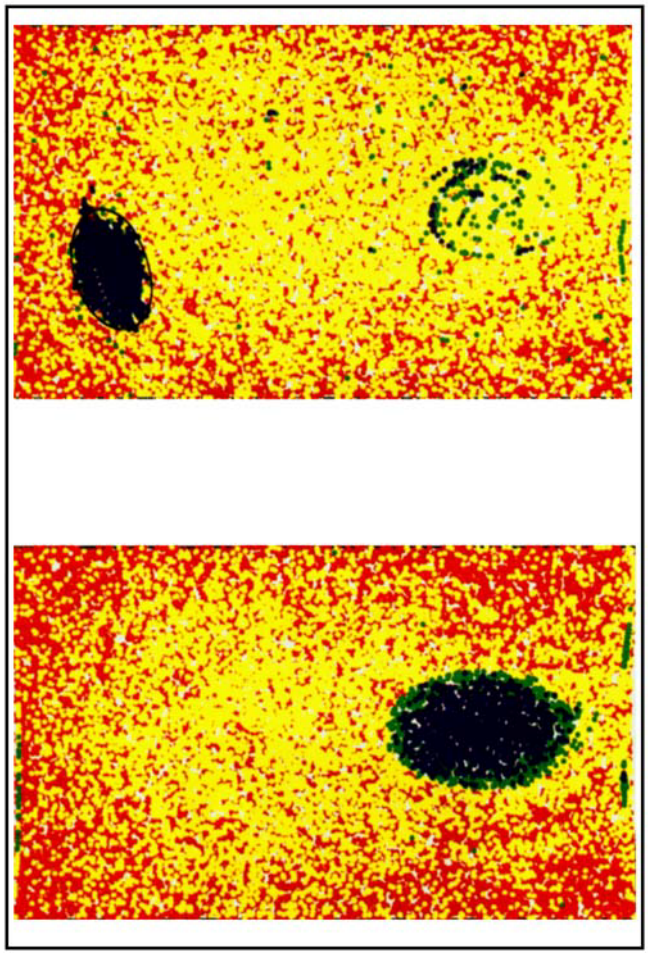

Figure 5. Stretching field λ without (upper) the fluid B minor phase body and with (lower) the fluid B minor phase body for $\sigma_B^* = 1.0$, $C_{\mu B} = 10.0$, $d_0 = 0.16L$, $(x_0, y_0) = (0.72L, 0.5H)$, $N = 20$, $A = 0.6$, $St = 0.16$ (black corresponds to log $\lambda <$ 1.0, green to 1.0 < log λ < 2.0, yellow to 2.0 < log λ < 5.5, and red to 5.5 < log λ < 15.0).

viscosity ratio effectively precluded significant circulation in fluid B, so stretching rates internal to the body remained very low. Stretching rates in the vicinity of the collapsed islands of Figure 4 were highly nonuniform, with some regions of low stretching persisting. This result can be attributed to the evident complexity of the KAM curve during the collapse.

The preceding results clearly indicate that a dissimilar minor phase body can effectively destroy islands and thereby improve mixing between similar fluids. Figures 3, 4 and 5 pertain to a single parametric condition in order to show in detail the events leading to island capture and island collapse. In Figures 6, 7 and 8, influences will be examined related to the size of the fluid B minor phase body, the initial proximity of this body to the eventual location of the island, the viscosity ratio, and the interfacial tension. In Figure 6, size and proximity are considered, and results are shown after the completion of ten periods ($N = 10$). Interfacial tension and viscosity ratio were identical to the values pertaining to the prior figures. The fluid B minor phase body was placed

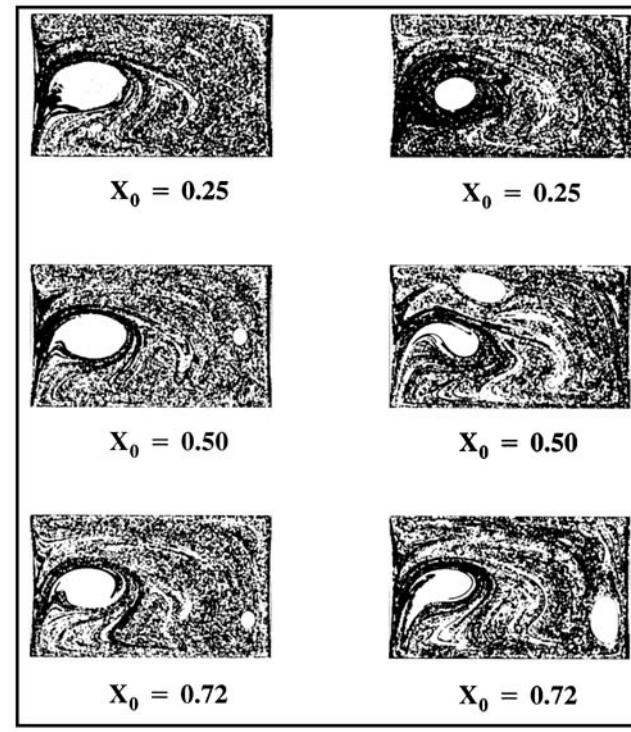

Figure 6. Influence of size (left column: $d_0 = 0.08L$; right column: $d_0 = 0.16L$) and initial location of fluid B minor phase body with $N = 10$, $A = 0.6$, $\sigma_B^* = 1.0$, $C_{\mu B} = 10.0$, $St = 0.16$.

at $x_0 = 0.25L$, $0.50L$, and $0.72L$ along the symmetric line $y_0 = 0.5H$. The diameters of the initially circular bodies were $0.08L$ and $0.16L$ for the left and right columns, respectively. Two fluid C bodies were initially located at $(x_1, y_1) = (0.08L, 0.5H)$ and $(x_2, y_2) = (0.85L, 0.5H)$. Results indicated that little influence on mixing between the similar fluids A and C occurred when the body of the dissimilar fluid B was small in comparison to the size of the island for all initial locations. This result can be easily understood by noting that the fluid B minor phase body can only modify the flow field in its vicinity. When small, it moved essentially as a passive body. For example, the fluid B minor phase body that was initially located inside the island ($x_0 = 0.25L$) remained inside the island as it moved although the island boundary was more disturbed. The influence on chaotic mixing of initial proximity to the island became much more appreciable when the fluid B body was of comparable size to the island. Interestingly, when located within the region eventually spanned by the island ($x_0 = 0.25L$) as shown in Fig. 1, the minor phase body replaced the island, with the active interface between fluids A and B serving effectively as a KAM surface. However, when the initial locations were beyond this region, the larger minor phase bodies induced greater instabilities in the island than did the smaller bodies, as shown in Figure 6. Further calculations indicated that the islands were destroyed at later mixing times, with greater times required for larger initial separation distances. From a practical point of view, a minor phase body of a dissimilar fluid or other suspended rigid body should be of comparable size to an island to destroy it.

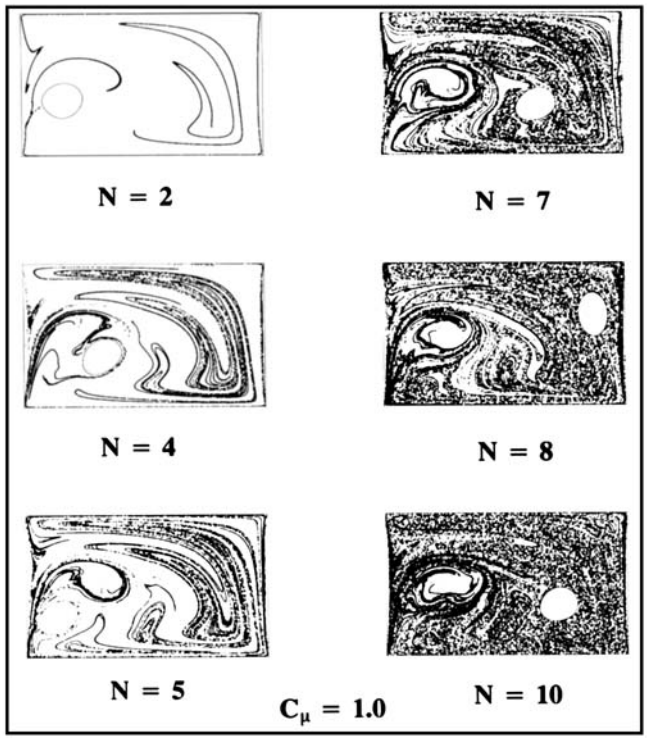

Figure 7. Evasion of fluid *B* minor phase body from the island at a lower viscosity ratio ($C_{\mu B} = 1.0$) with $A = 0.6$, $\sigma_B^* = 1.0$, $d_0 = 0.16L$, and $(x_0, y_0) = (0.25L, 0.5H)$.

The influence of the viscosity ratio $C_{\mu B}$ $(= \mu_B/\mu_A)$ was also considered. Computations were performed for $0.5 < C_{\mu B} < 10.0$ with other conditions identical to those in Figures 3–5. The fluid B minor phase body was initially placed at $(x_0, y_0) = (0.25L, 0.5H)$, which was the eventual location of the island in Figure 2. In Figures 3 and 6, it was demonstrated that such a minor phase body with $C_{\mu B} = 10.0$ can replace an island. Results for $C_{\mu B} = 1.0$ are shown in Figure 7. Unlike in Figure 3, the minor phase body evades the forming island, as revealed by careful inspection of the individual panels for $N = 2$, $N = 4$, and $N = 5$. The simultaneous formation of the island and the movement of the body away from the island are evident at higher mixing periods. As in Figure 6, the island boundary was greatly distorted at the completion of ten mixing periods. Due to this evasion from the island and induced flows external to the island by the moving body, the island does not persist. Calculations indicated that the island was subsequently destroyed in a fashion similar to the one shown in Figure 4, for the case where the body was placed initially away from the eventual location of the island. In general, with $C_{\mu B} \geq 4.0$, a minor phase body of similar size to the island can effectively destroy the island.

Results for various interfacial tensions between fluid B and similar fluids A and C are shown in Figure 8. For $\sigma_B^* \geq 0.5$, the island was destroyed and good mixing was achieved in the similar fluids. However, as σ_B^* was decreased, the boundary of the island became distorted, but a large island persisted even at the completion of twenty mixing periods ($N = 20$). For small σ_B^*, the fluid B minor phase body was more readily deformed so that alterations to the flow field and chaotic

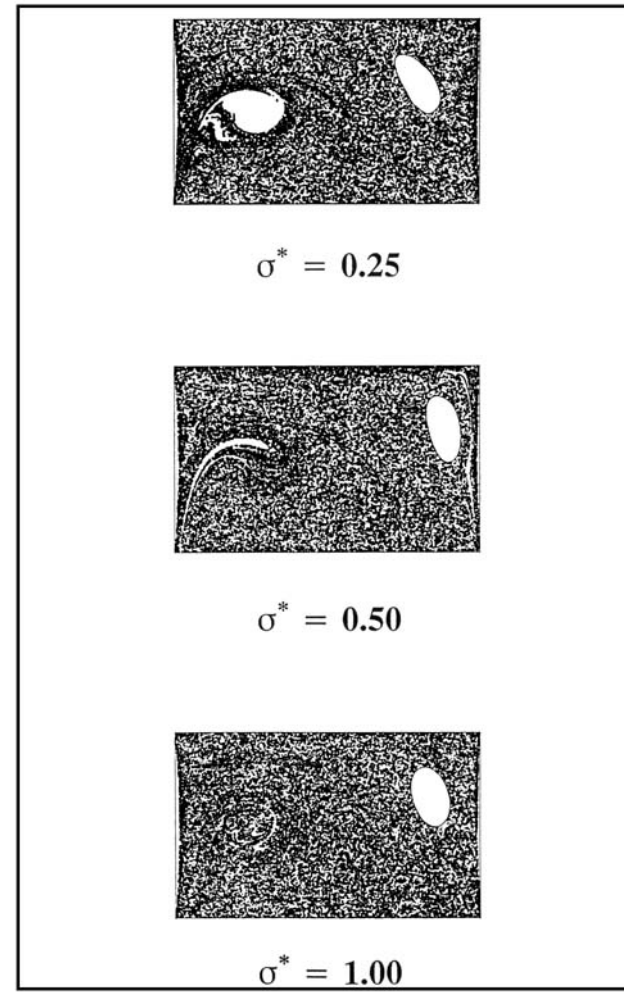

Figure 8. Influence of interfacial tension on island collapse with $N = 20$, $A = 0.6$, $C_{\mu B} = 10.0$, $d_0 = 0.16L$, and $(x_0, y_0) = (0.72L, 0.5H)$.

mixing conditions between the similar fluids A and C were lessened. It is evident from these results that minor phase bodies with large interfacial tensions more effectively destabilize islands.

Conclusions

The motion of a dissimilar fluid minor phase body can sufficiently alter time-dependent flow fields such that islands within similar fluids are destroyed. Island collapse can occur even when such bodies are located initially away from the eventual location of an island. Alternately, if the minor phase body of dissimilar fluid is of comparable size to an island and located initially near an eventual island location, an island may be effectively replaced by the advecting body. Islands persist in the presence of dissimilar fluid minor phase bodies for longer times at lower viscosity ratios and lower interfacial tensions and may be unaffected when the minor phase bodies are small in comparison to the island. In industrial mixing processes where several fluids are commonly combined, results suggest that mixing between similar fluid phases is promoted in the presence of a dissimilar fluid. When similar flu-

ids are mixed, a dissimilar fluid may be introduced to promote mixing and later removed using a simple separation process. Results clearly demonstrate the limitations of mixing studies where only similar fluids are used. While such studies can disclose many interesting aspects of mixing, local mixing conditions may not be accurately predicted. Efforts of designers to improve the performance of commercial mixers and extruders should include multiphase numerical and experimental models whenever possible to further clarify mixing conditions or to suggest possible outcomes.

Acknowledgments

Support for this work was provided by the National Science Foundation under grant CMS-9253640 in conjunction with a Presidential Faculty Fellow Award to one of the authors (D. A. Z.), and is gratefully acknowledged.

Notation

A = aspect ratio of the mixing cavity = H/L
C_μ = ratio of viscosity of minor phase fluid B to the viscosity of the major phase fluid $A = \mu_B/\mu_A$
C_ρ = ratio of density of minor phase fluid B to the density of the major phase fluid $A = \rho_B/\rho_A$
d_0 = diameter of the initially circular minor phase body of fluid B (m)
H = height of mixing cavity
N = number of periods, where one period comprises the movement of both cavity walls
P = dimensionless pressure = p/P_0
P_0 = scale factor for pressure = $\mu_A u_0 L$
p = pressure (N/m^2)
Re = Reynolds number = $\rho_A u_0^2 T/\mu_A$
t = time (s)
T_0 = scale factor for time = L/u_0
u = velocity component in x-direction (m/s)
u_0 = scale factor for velocity equivalent to the constant nonzero speed of the moving walls (m/s)
U = dimensionless velocity component in x-direction = u/u_0
v = velocity component in y-direction (m/s)
V = dimensionless velocity component in y-direction = v/u_0
x = horizontal coordinate (m)
x_0 = initial x-location of a minor phase body (m)
X = dimensionless horizontal coordinate = x/L
y = vertical coordinate (m)
y_0 = initial y-location of a minor phase body (m)
Y = dimensionless vertical coordinate = y/H

Greek letters

μ = dynamic viscosity (kg/m·s)
ρ = mass density of fluid (kg/m^3)
σ = interfacial tension (N/m)
σ^* = dimensionless interfacial tension = $\sigma/\mu_A u_0$
τ = dimensionless time = t/T_0
κ = curvature of fluid–fluid interface (1/m)
K = dimensionless curvature of fluid–fluid interface = κL

Literature Cited

Aref, H., "Stirring by Chaotic Advection," *J. Fluid Mech.*, **143,** 1 (1984).
Bentley, B. J., and L. G. Leal, "A Computer-Controlled Four-Roll Mill for Investigations of Particle and Drop Dynamics in Two-Dimensional Linear Shear Flows," *J. Fluid Mech.*, **167,** 219 (1986).
Brackbill, J. U., D. B. Kothe, and C. Zemach, "A Continuum Method for Modeling Surface Tension," *J. Comp. Phys.*, **100,** 335 (1992).
Chakravarthy, V. J., and J. M. Ottino, "Mixing of Two Viscous Fluids in a Rectangular Cavity," *Chem. Eng. Sci.*, **51,** 3613 (1996).
Chien, W.-L., H. Rising, and J. M. Ottino, "Laminar Mixing and Chaotic Mixing in Several Cavity Flows," *J. Fluid Mech.*, **170,** 355 (1986).
Hirt, C. W., and B. D. Nichols, "Volume of Fluid (VOF) Method for the Dynamics of Free Boundaries," *J. Comp. Phys.*, **39,** 201 (1981).
Jana, S. C., M. Tjahjadi, and J. M. Ottino, "Chaotic Mixing of Viscous Fluids by Periodic Changes in Geometry: Baffled Cavity Flow," *AIChE J.*, **40,** 1769 (1994).
Kothe, D. B., R. C. Mjolsness, and M. D. Torrey, "RIPPLE: A Computer Program for Incompressible Flows with Free Surfaces," Los Alamos National Laboratory Report LA-12007-MS, Los Alamos, NM (1991).
Leong, C. W., and J. M. Ottino, "Experiments on Mixing Due to Chaotic Advection in a Cavity," *J. Fluid Mech.*, **209,** 463 (1989).
Leong, C. W., "Chaotic Mixing of Viscous Fluids in Time-Periodic Cavity Flows," PhD Diss., Univ. of Massachusetts, Amherst (1990).
Lichtenberg, A. J., and M. A. Lieberman, *Regular and Stochastic Motion*, Springer-Verlag, New York (1992).
Liu, M., R. L. Peskin, and F. J. Muzzio, "Fractal Structure of a Dissipative Particle-Fluid System in a Time-dependent Chaotic Flow," *Phys. Rev. E*, **50,** 4245 (1994a).
Liu, M., R. L. Peskin, F. J. Muzzio, and C. W. Leong, "Structure of the Stretching Field in Chaotic Cavity Flows," *AIChE J.*, **40,** 1273 (1994b).
Liu, Y. H., and D. A. Zumbrunnen, "Emergence of Fibrillar Composites Due to Chaotic Mixing of Molten Polymers," *Poly. Compos.*, **17,** 187 (1996).
Muzzio, F. J., M. Tjahjadi, and J. M. Ottino, "Self-Similar Drop Size Distributions Produced by Breakup in Chaotic Flows," *Phys. Rev. Lett.*, **67,** 54 (1991).
Ottino, J. M., *The Kinematics of Mixing: Stretching, Chaos, and Transport*, Cambridge Univ. Press, Cambridge, England (1989).
Patankar, S. V., *Numerical Heat Transfer and Fluid Flow*, Hemisphere, New York (1980).
Richards, J. R., A. N. Beris, and A. M. Lenhoff, "Steady Laminar Flow of Liquid-Liquid Jets at High Reynolds Numbers," *Phys. Fluids*, **A5,** 1703 (1993).
Souvaliotis, A., S. C. Jana, and J. M. Ottino, "Potentialities and Limitations of Mixing Simulations," *AIChE J.*, **41,** 1605 (1995).
Spalding, D. B., "A Novel Finite Difference Formulation for Differential Expressions Involving Both First and Second Derivatives," *Int. J. Numer. Mech. Eng.*, **4,** 551 (1972).
Stone, H. A., and L. G. Leal, "Relaxation and Breakup of an Initially Extended Drop in an Otherwise Quiescent Fluid," *J. Fluid Mech.*, **198,** 399 (1989).
Stone, H. A., "Dynamics of Drop Deformation and Breakup in Viscous Fluids," *Annu. Rev. Fluid Mech.*, **26,** 65 (1994).
Tjahjadi, M., and J. M. Ottino, "Stretching and Breakup of Droplets in Chaotic Flows," *J. Fluid Mech.*, **232,** 191 (1991).
Tiahiadi, M., H. A. Stone, and J. M. Ottino, "Satellite and Subsatellite Formation in Capillary Breakup," *J. Fluid Mech.*, **243,** 297 (1992).
Zhang, D. F., "Development of Interfacial Morphologies During the Chaotic Mixing of Fluids," PhD Thesis, Clemson Univ., Clemson, SC (1996).
Zhang, D. F., and D. A. Zumbrunnen, "Influences of Fluidic Interfaces on the Formation of Fine Scale Structures by Chaotic Mixing," *J. Fluids Eng.*, **118,** 40 (1996).
Zumbrunnen, D. A., K. C. Miles, and Y. H. Liu, "Auto-Processing of Very Fine-Scale Composite Materials by Chaotic Mixing of Melts," *Composites Part A*, **27A,** 37 (1996).

Manuscript received Dec. 8, 1995, and revision received June 6, 1996.